MRS Advances
https://doi.org/10.1557/s43580-024-01028-3

ORIGINAL PAPER

Ab-initio study of the transition pathways for single and double interstitial solute (H, N, O, H-H, N-N, and O-O) within bcc refractory metals (Mo and Nb)

Henry Elorm Quarshie[1] · Henry Martin[1,2] · Eric Kwabena Kyeh Abavare[1] · Alessandra Continenza[3]

Received: 22 August 2024 / Accepted: 26 November 2024

Abstract

Transition pathways of single (Hydrogen (H), Nitrogen (N), and Oxygen (O)) and double (H-H, N-N and O-O) interstitial solutes within bcc refractory metals (molybdenum (Mo) and niobium (Nb)) were investigated. This work is crucial for understanding how atmospheric gases, rich in H, O, and N, interact with metals. Ab-initio calculations for equilibrium and structural parameters, dissolution energetics, charge transfers, minimum energy path, and diffusion coefficients were performed. Single solutes exhibited preferential occupancy sites, with H favoring tetrahedral sites (t-sites), N preferring octahedral sites (o-sites), and O showing material-dependent behavior. The energy barriers for single solute diffusion ranged from 0.10 to 1.34 eV, aligning with experimental findings. Double interstitial solutes significantly reduced activation energies (E_a), leading to faster diffusion for all configurations except for MoO. This effect is due to the second solute's influence on repulsive/attractive forces and local lattice relaxations, altering preferred diffusion pathways.

Introduction

Refractory metals (V, Cr, Nb, Mo, Ta, W, Re, and others) are highly valued in industrial applications due to their exceptional strength and high-temperature stability [1]. This physical property makes them suitable for hot metallurgical applications, furnace technology, nuclear power systems, and aerospace applications. In many of these applications, refractory metals are utilized as alloying elements to impart their superior properties to other materials.

Despite their inherent strength and stability, the performance of refractory metals can be further tailored by introducing foreign solutes which significantly impact their mechanical properties [2].

✉ Henry Elorm Quarshie
hequarshie2@st.knust.edu.gh

Henry Martin
hmartin@knust.edu.gh

[1] Department of Physics, Kwame Nkrumah University of Science and Technology, Kumasi, Ghana

[2] Center for Scientific and Technical Computing, National Institute for Mathematical Sciences, Kumasi, Ghana

[3] Dipartimento di Scienze Fisiche e Chimiche, Universitá degli studi dell'Aquila, L'Aquila, Italy

While substitutional solid solutions have been extensively studied, the fascinating realm of interstitial solid solutions has received less attention. Recent research has shed light on the intriguing role of interstitial solutes (B, C, N, and O) in bcc transition metals. These solutes have been shown to stabilize the core configuration of screw dislocations, influencing their motion and ultimately affecting plasticity. Similar observations have been made in bcc refractory metals (V, Nb, Ta, Mo, and W) with C and O [3]. Furthermore, interstitial solutes significantly increase bcc metal's ductile-to-brittle transition temperature (DBTT). The influence of interstitial solutes extends beyond their individual effects. For instance, adding O and N to high-purity Nb and Ta crystals can induce hardening. Conversely, studies have shown decreased Nb hardness with increasing O concentration [4]. These observations suggest a complex interplay between different interstitial solutes, their combined influence on dislocation motion, and the material's ability to undergo plastic deformation.

Given the critical role of bcc refractory metals in diverse applications, understanding the diffusion and stability of interstitial atoms and their role across various regimes and scales is paramount. For instance, the investigation of diffusion H isotopes (deuterium (D) and tritium (T)) in Mo reveals the underlying migration mechanisms and their potential implications for nuclear technology, hydrogen

Published online: 09 December 2024

storage, and fuel cell applications [5]. Furthermore, the diffusion of H and He in Mo demonstrates the critical role in enhancing diffusion mechanisms in bcc refractory metals by providing lower-energy migration pathways [6].

This work investigates the diffusion pathways of single and double interstitial solutes (H, N, O, H-H, N-N, O-O) in the bcc lattices of molybdenum (Mo) and niobium (Nb), similar to how atmospheric gases interact with these metals. Beyond individual diffusion pathways, it explores how an additional interstitial atom affects diffusion mechanisms. The "double interstitials" concept adds complexity, helping to understand solute interactions with each other and the host lattice. Using ab-initio calculations, this study reveals how one interstitial atom influences the energy landscape and preferred diffusion pathways, which is crucial for understanding the mechanical properties of bcc refractory metals.

Computational method

First-principle simulations were performed using Density Functional Theory (DFT) within the Vienna ab-initio simulation package (VASP) [7]. Semi-core p states were treated as valence electrons in the PAW pseudopotential framework [8], and the PBE-GGA approximation was used for exchange-correlation functional.

According to Kresse and Furthmüller [9] to ensure accuracy of the results in this work, a careful computational study was performed to optimize the values of the parameters involved to reach convergence. A plane wave energy cutoff of 600 eV was set, with a Monkhorst-Pack **k**-mesh grid of 8×8×8 for X_2 and 3x3x3 for X_{16}, X_{54}, and X_{128}, where X represents Mo and Nb, and the subscript denotes the total number of atoms in the system. The Methfessel-Paxton smearing method [10] was used with a smearing width of 0.2 eV to keep entropy below 1 meV/atom. Supercells ranging from 1x1x1 to 4x4x4 were constructed, and dimer calculations were performed in a cubic cell with Γ point calculation. The Broyden's method [11] was applied for final charge mixing, and the Conjugate Gradient (CG) method was used for structural relaxation until atomic forces were below 10^{-6} eV/atom.

For interstitial calculations, a single interstitial atom (H, N, or O) was either inserted in an octahedral or tetrahedral site (o-site or t-site), and another one placed in a relative stable site for the double interstitial structure analysis (see Fig. 1 a). All supercells were fully relaxed to forces lower than 0.01 eV/Å. The equation to evaluate the stability of interstitial atoms is written as

$$E_{d_x} = E(X_nY) - E(X_n) - \frac{1}{2}E(Y_2) \tag{1}$$

where, E_{d_x} is the dissolution energy with a solute atom either at the o- or t-site (thus, $x = $ o or t). X_n is the bulk bcc refractory metal (Mo or Nb) without any interstitial atom and with total energy $E(X_n)$. $E(X_nY)$ is the total energy of the bulk structure with an interstitial atom. Finally, $E(Y_2)$ is the energy of the molecule (H_2, N_2, O_2), where Y is either H, O, or N. For energies involving lighter atoms as in the case of H, the zero-point energy ($E_{\mathrm{ZPE}} = \frac{1}{2}\Sigma h\nu$) must be considered, where ν is the real normal mode frequency.

The Climbing-Image Nudged Elastic Band (CI-NEB) method [12] was used to find the minimum energy path (MEP). All transition simulations were achieved using the same convergence parameters. Figure 1 b, illustrates transition pathways considering three **o**- and **t**-sites. The transitions are **o**-**o** (**o**-site to another nearest **o**-site), **o**-**t**, **t**-**o**, **t**-**t,** and **t**-**o**-**t**, shown in the figure as a-c, a-b, d-e, b-d, and b-c-f, respectively.

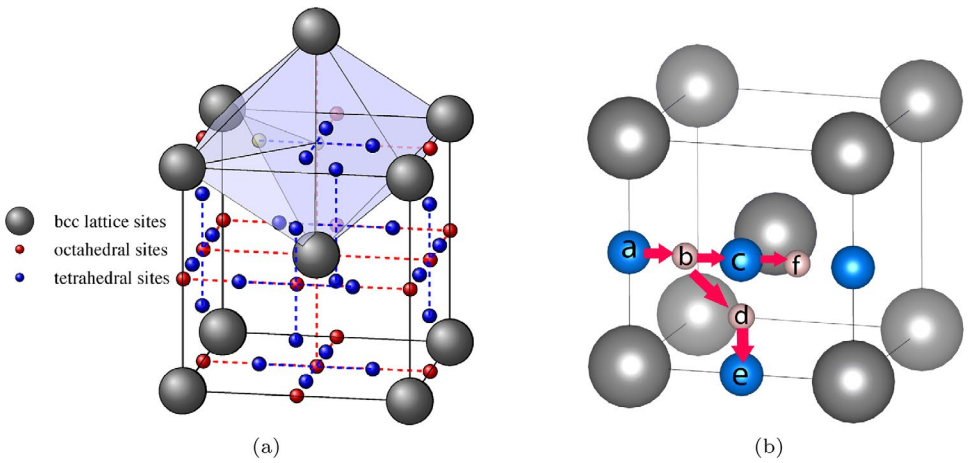

Fig. 1 **a** BCC lattice cell of o- and t-sites **b** Positions and transitions of interstitial atoms along given paths, o-o (o-site to the nearest o-site), t-t, o-t, t-o, and a second type of t-t (t-o-t)

Results and Discussion

The thermodynamic stable sites were calculated to determine the optimum transition paths of the solute atoms within the interstitial sites of the bcc refractory metals. The lattice constants and the bulk modulus of Mo were calculated to be 3.16 Å and 264 GPa, respectively, and that of Nb was estimated to be 3.325 Å and 168 GPa. These values are in agreement with literature [13–15] and are presented in the supplementary material (ESM_1) alongside the results of vibrational frequencies for the dimers (H_2, N_2, and O_2).

Solubility

The dissolution energy difference $\Delta E_{d\ o-t}$, as derived from Eq. 1, serves as the initial step in assessing the stability of solute atoms (H, N, and O) within bcc refractory metals, Mo and Nb at the o-site and t-site. A positive $\Delta E_{d_{o-t}}$ indicates that the t-site is more stable, while a negative value signifies the o-site as the preferred location.

For H, the results reveal a general preference for the t-site across all relaxed structures, except for Mo_2H (33.3 at.%). The dissolution energies for H in the t-site of Mo_nH structures range from 0.5 to 0.8 eV (midpoint value of 0.62 eV), indicating an endothermic dissolution process, consistent with previous findings of 0.62 eV [16]. In contrast, H in Nb exhibits exothermic behavior at both the o-site and t-site, with a preference for the t-site.

Nitrogen prefers the o-site in both Mo and Nb structures, with dissolution energies indicating an endothermic process in Mo and an exothermic process in Nb. The oxygen solute favors the t-site in Mo structures, except for Mo_2O, while in Nb, O prefers the o-site. The dissolution mechanism is generally exothermic in both Mo and Nb, with a few exceptions for o-site $Mo_{16}O$ and t-site Mo_2O). Further details on the tables can be found in the supplementary material (ESM_1).

The variation in site energies within a specific solid structure is directly connected to the lattice distortion caused by the interstitial solute which arises from the solute concentration [17].

Lattice distortions

Interstitial solute atoms (H, O, N) in a crystal lattice cause localized distortions, impacting the material's properties, particularly the diffusion behavior [18]. The degree of distortion depends on the specific interstitial atom and its site within the lattice [17]. The distortions observed in this work are measured for the nearest neighbor (NN) atoms relative to the transitioning interstitial atom for both the single and double interstitial structures. This allows us to identify prolate or oblate tetragonal distortions [18]. For example Fig. 2 illustrates a nitrogen transition from an o-site (a and d) through a t-site (b and e) and then to an o-site (c and f), i.e., a "o-t-o". During this path, the bcc lattice undergoes significant tetragonal distortion along the [001] direction for the single interstitial structures. For the double interstitial structures, it is observed that the presence of the second interstitial atom at the second nearest neighbor (NN) o-site induces a distortion along the [010] direction of its first NN host atoms. This, in turn, causes a slight distortion (1.1 mÅ) along the [101] of the transition interstitial atom, thereby altering the original transition path. Similar trend was observed for all structures with double interstitial atoms and various sites. Further analysis is presented in Table 1

For H in Mo, the average distortions ($\bar{d}$ in units of 10^{-1} Å) were relatively small and localized around the interstitial site, with the largest values in the [010] and [001] directions for both single (0.75) and double (1.27) interstitial structures. In Nb, distortions were more pronounced, especially in double interstitial structures along the [100] (4.01) and [001] (3.73) directions, and decreased significantly with distance from the interstitial site. Nitrogen at the o-site caused substantial prolate distortions in both Mo (3.59 for single and 5.07 for double) and Nb (3.92 for single and 4.47 for double), with stronger effects in Nb. Oxygen at the t-site in Mo exhibited notable prolate and oblate distortions, with double interstitials showing larger overall effects. In the o-site of Nb, substantial distortions are present in both single and

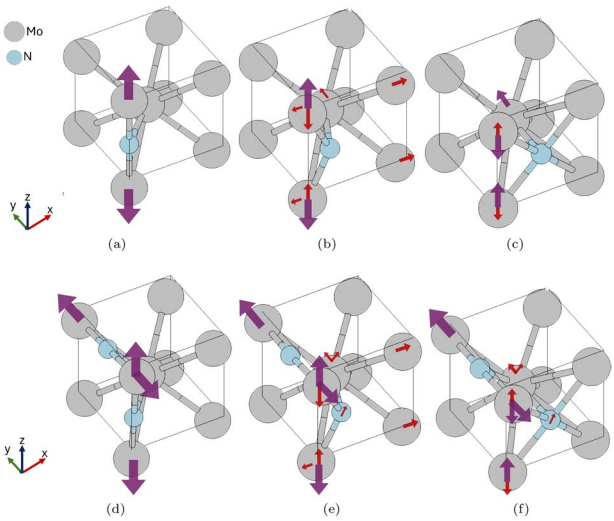

Fig. 2 Nitrogen (blue ball) transition from an o-site to another o-site through a t-site in Mo (gray ball). **a** single interstitial at o-site **b** single interstitial at t-site, a transition state, **c** single interstitial at the final o-site, **d** double interstitial at o-site, **e** double interstitial with the transitioning atom at the t-site, **f** double interstitial with the transitioning atom at the final o-site. Arrows show the extent and direction of distortions, red for small displacements, and purple for large displacements

double interstitial structures, demonstrating strong prolate effects. The significant distortions in farther neighbors in both Mo and Nb highlight the broad impact of O interstitials.

The contour plots shown in Fig. 3 provide a clear visualization of the displacement fields caused by the interstitial atoms (H, N, O) in Mo structures, illustrating how these atoms influence the surrounding Mo lattice. Corresponding plots for Nb structures are available in the supplementary material.

In general, double interstitial structures exhibited larger distortions than single interstitials, demonstrating the additive effect of multiple interstitials on the lattice.

Charge transfers

In this work, the charge transfer and distribution for interstitial atoms within Mo and Nb lattices were analyzed using 128 atomic structures (X_{128}). The Bader charge analysis reveals that these interstitial atoms acquire electrons from the host atoms, resulting in negatively charged interstitials at both o- and t-sites, with minimal charge differences. H atoms in both o-site and t-site positions exhibit similar trends in charge transfer, with the nearest neighbor (1NN) host atoms providing more electrons than the second nearest neighbor (2NN) host atoms. This pattern is consistent for N and O atoms as well, indicating that the interaction between interstitials and host atoms is strongest with the 1NN atoms. This interaction combines ionic and covalent bonding characteristics, with the dominant ionic component arising from significant charge transfer. Further details on the Bader charge values and the charge density difference plots can be found in the supplementary material (ESM_1).

Diffusion

This section discusses the diffusion of the interstitial atoms in dilute solutions, where single and double interstitial solutes were considered for the 4x4x4 unit structure (128 host atoms).

Single interstitial atom

The activation energies for the diffusion of single and double interstitial atoms in Mo and Nb are presented in Table 2. We first consider H diffusion in Mo and Nb as jumps between 1NN t-sites with activation energy of $E_a = 0.16$ eV. This aligns well with both theoretical (0.16 eV [6, 16]) and experimental findings (0.17 eV [19]). The minor discrepancies observed might be attributed to the presence of vacancies and other defects in experimental samples, as reported [16]. That of H in Nb was also calculated to be $E_a = 0.15$ eV, which is in reasonable agreement with experimental values reported at low temperatures. Nitrogen diffusion in both metals occurs through jumps between o-sites with the TS residing in a t-site (Fig. 4a). The activation energies were calculated as 0.65 eV for Mo and 1.34 eV for Nb, consistent with experimental values [20, 21]. For O diffusion in Mo, the preferred path between t-sites as shown in Fig. 4b has an activation energy of 0.1 eV, indicating rapid diffusion at high temperatures. A second path involving a jump through an o-site has a higher activation energy of 0.15 eV, suggesting it is less favorable. In Nb, O diffuses similarly to N, with an activation energy of 0.97 eV, reflecting a jump from one o-site

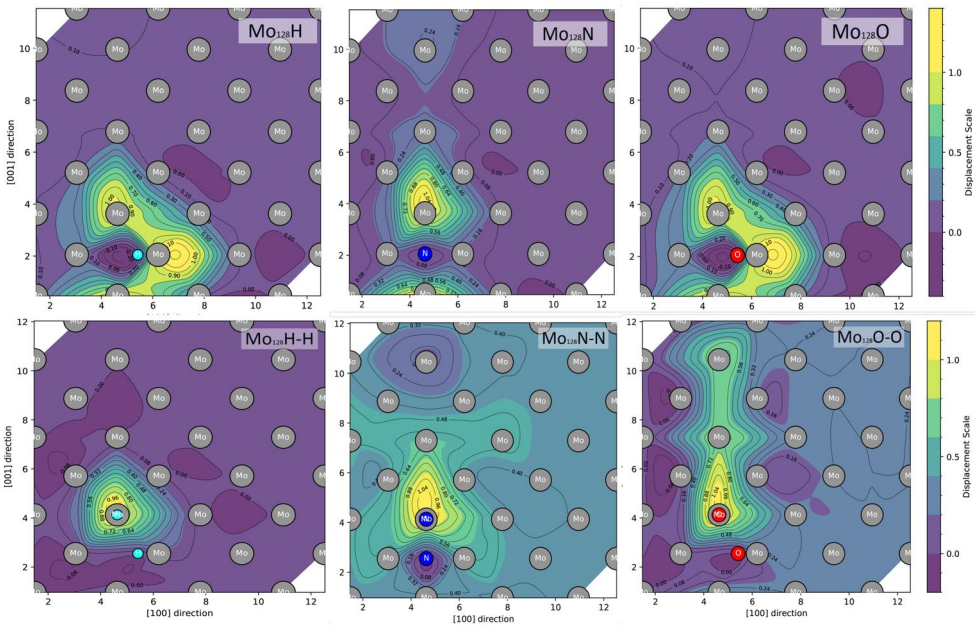

Fig. 3 Contour plots of the lattice distortions due to the presence of single and double interstitial atoms in Mo. Distortion magnitudes were normalized (0 to +1.0) for better representation

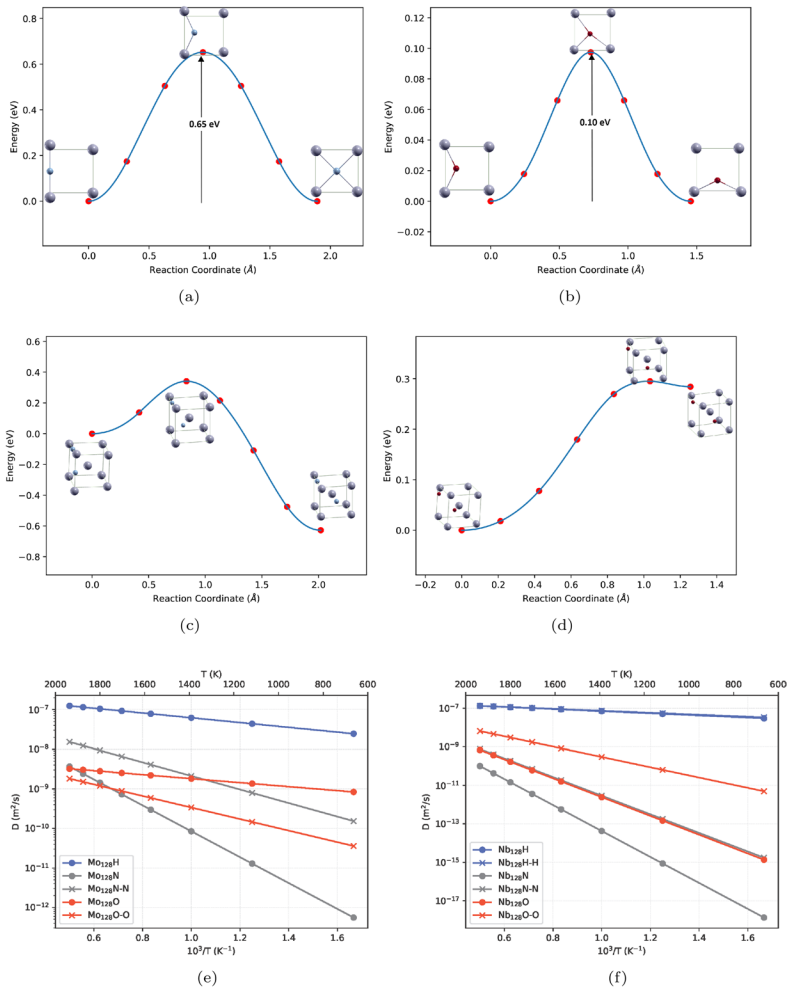

Fig. 4 NEB calculations of **a** single N in Mo, o-t-o path, **b** single O in Mo, t-t path, **c** double N in Mo, o-t-o path, **d** double O in Mo, the t-t path, and diffusion coefficients of single and double interstitials in **e** Mo and **f** Nb, as a function of reciprocal temperature

Table 1 Average distortion, $\bar{d}$ (in 10^{-1} Å), of the first to fourth nearest neighbor (NN) host atoms at 0 K, along the [100], [010], and [001] directions for the single/double interstitial structures

Specie	Site	Mo			Nb		
		$\bar{d}_{[100]}$	$\bar{d}_{[010]}$	$\bar{d}_{[001]}$	$\bar{d}_{[100]}$	$\bar{d}_{[010]}$	$\bar{d}_{[001]}$
H_t	1NN	0.16/0.26	0.75/1.19	0.75/1.27	0.21/4.01	0.77/0.95	0.77/3.73
	2NN	0.08/0.12	0.07/0.17	0.07/0.71	0.06/0.15	0.09/4.21	0.09/0.33
	3NN	0.02/0.06	0.08/0.12	0.08/0.17	0.05/4.15	0.14/0.25	0.14/2.86
	4NN	0.02/0.02	0.01/0.06	0.01/0.07	0.05/0.15	0.03/0.17	0.03/0.14
N_o	1NN	0.52/1.02	0.52/1.02	3.59/5.07	1.09/1.97	1.09/1.97	3.92/4.47
	2NN	0.25/0.20	0.25/0.36	0.57/0.25	0.19/0.41	0.19/0.17	0.90/0.69
	3NN	0.13/0.22	0.13/0.58	0.83/0.64	0.32/0.58	0.32/0.75	0.96/0.75
	4NN	0.05/0.07	0.05/0.19	0.19/0.25	0.28/0.33	0.28/0.04	0.32/0.53
$O_{t/o}$	1NN	0.61/6.13	2.01/2.74	2.01/4.55	0.60/0.63	0.60/0.63	4.01/4.87
	2NN	0.09/0.36	0.19/6.15	0.19/0.97	0.17/0.35	0.17/0.40	0.85/0.41
	3NN	0.05/6.33	0.35/0.69	0.35/6.26	0.26/0.41	0.27/0.75	0.99/0.74
	4NN	0.05/0.25	0.03/6.38	0.03/0.14	0.23/0.27	0.23/0.17	0.35/0.53

X_n - where X and n are the interstitial atom and its stable site, respectively

Table 2 Activation energy (E_a, in eV) and prefactor (D_0, in $10^{-6}m^2s^{-1}$) of the diffusion coefficients of single and double interstitial solute atom (where n=128). ZPE correction in brackets

Structure	Path	E_a			D_o		
		This work	Ref	Ref	This work	Ref	Ref
Mo_nH	t→t	0.16(0.12)	0.17[a]	0.16[b](0.12[d])	0.29(0.25)	–	0.29[b]
Mo_nN	o→t→o	0.65	1.20[e]	1.08[f]	0.16	0.3[e]	–
Mo_nO	t→t	0.10	0.05[g]	–	0.058	0.041[g]	–
Nb_nH	t→t	0.15(0.11)	0.068[c]	–	0.29(0.25)	0.009[c]	–
Nb_nN	o→t→o	1.34	1.67[c]	1.08[h]	0.24	6.30[c]	0.23[h]
Nb_nO	o→t→o	0.97	1.11[c]	–	0.19	0.43[c]	–
Mo_nN-N	o→t→o	0.34	–	–	0.11	–	–
Mo_nO-O	t→t	0.29	–	–	0.01	–	–
Nb_nH-H	t→t	0.14(0.1)	–	–	0.29(0.24)	–	–
Nb_nN-N	o→t→o	0.96	–	–	0.20	–	–
Nb_nO-O	o→t→o	0.53	–	–	0.14	–	–

[a]Ref.[19] [b]Ref.[16] [c]Ref.[20] [d]Ref.[6] [e]Ref.[21] [f]Ref.[24] [g]Ref.[25] [h]Ref.[26]

to another via a t-site. Next, the diffusion coefficients (D) of solute atoms in the selected refractory metals are determined using the Arrhenius diffusion equation:

$$D(T) = D_0 \exp(-E_a/kT), \tag{2}$$

where D_0 and E_a are the pre-exponential factor and the activation energy of solute atom, respectively. The value of D_0 is expressed as $D_0 = \frac{1}{6}a^2\nu$, for a cubic structure, where ν is the vibration frequency and a is the lattice constant [22]. To get a good approximation of the ν value, Wert and Zener [22] in their theory estimated $\nu = \sqrt{2E_a/ma^2}$. Here, m is the mass of the solute atom being considered. It is crucial to consider quantum corrections for light elements like H to accurately express the diffusion coefficient. This is written as

$$D(T) = D_0^{'} \exp(-(E_a + \Delta E_{\mathrm{ZPE}})/kT), \tag{3}$$

where $D_0^{'}$ is the pre-exponential factor with the zero-point correction, which is expressed as $\frac{1}{6}a^2\sqrt{2(E_a + \Delta E_{\mathrm{ZPE}})/ma^2}$. ΔE_{ZPE} is the zero-point energy (ZPE) difference between the saddle point and minimum energy configuration, which is −0.043 and −0.042 eV for H in Mo and Nb, respectively. This reduces the activation energies to 0.12 and 0.11 eV, which is similar to experimental values obtained by McNeil et al [23]. Table 2 summarizes the diffusion parameters, thus, the activation energies E_a and pre-exponential factor D_0 of all structures.

The diffusion coefficients (D) for temperatures ranging from 600 K to 2000 K (Fig. 4e, f) closely align with literature values [6, 20]. H has the highest diffusion coefficient among the three elements in both Mo and Nb, indicating faster lattice traversal than N and O. N moves slower than H but faster than O, consistent with theoretical and experimental studies, despite slight value discrepancies within acceptable error margins.

Double Interstitial atoms

This subsection examines how the presence of a second, identical interstitial solute atom within the Mo and Nb structures influences the diffusion of the first solute atom. We again focus on the three specific solute types: hydrogen (H), nitrogen (N), and oxygen (O).

For each solute type, we consider identical distances (H-H, N-N, and O-O) between the solute atoms and their potential stable sites within the Mo and Nb lattices. It is essential to address the potential formation of interstitial dimers such as H_2, O_2, and N_2. Evidence suggests that the formation of such dimers is unlikely under the conditions studied in this work [16]. Detailed analysis of the interstitial dimer formation is provided in the supplementary material (ESM_1).

Similar to the investigation of a single solute atom, we employ the same transition pathways to simulate the movement of a single solute atom within the structures in the presence of another. However, it is important to note that some calculations did not reach a stable configuration (specifically the MoH-H t-t transition). The additional solute atom distorts the surrounding lattice, impacting the transition states (TS) involved in diffusion for most configurations.

Interestingly, apart from the slight shift in the TS sites (i.e., position displacement), a notable decrease in the activation energy for the diffusion process of the first solute atom was observed for all configurations except MoO (Table 2). For instance, the transition energy for MoN dropped from 0.65 eV for a single interstitial atom to 0.34 eV when an additional solute was introduced at a 2NN stable site. Similar reductions were observed for NbH, NbN, and NbO, with their transition energies decreasing from 0.15 eV, 1.34 eV, and 0.97 eV to 0.14 eV, 0.96 eV, and 0.53 eV, respectively.

The reduction in activation energy can be attributed to the influence of the second solute atom on the repulsive

(attractive or mix) interactions experienced by the first solute within the lattice. Typically, solute atoms experience repulsion (attraction) from the surrounding host lattice atoms, creating an energy barrier that hinders their diffusion [20]. However, the presence of a second solute can create a more favorable diffusion environment for the first by partially relieving these repulsive (attractive) forces through two distinct mechanisms: (1) Local lattice relaxation induced by the second solute reduces the distortion and repulsive forces around the first solute. This creates a more accommodating environment for the first solute's movement through the lattice. (2) Strain sharing between the two solutes effectively lowers the overall energy barrier for the first solute's diffusion by redistributing the mechanical stress within the lattice.

The observed reduction in activation energy directly translates to an expected increase in the diffusion rate of the interstitial solute. Figure 4e, f depicts a plot of the diffusion coefficient by considering temperature range of 600 K to 2000 K in comparison to the single interstitial atom systems.

Conclusion

The ab-initio calculations employed to investigate the fundamental properties of H, N, O, H-H, N-N, and O-O within two (2) bcc refractory metals from Groups VB (niobium (Nb)) and VIB (molybdenum (Mo)) of the periodic table. This work revealed preferential occupancy sites for each single interstitial solute: H favored tetrahedral sites (t-sites) in both Mo and Nb, while N preferred octahedral sites (o-sites) in both. O exhibited a material-specific preference, occupying t-sites in Mo and o-sites in Nb. This difference is likely linked to the individual deformation behaviors observed in these Group VB and VIB metals. Furthermore, the diffusion of single and double interstitial solutes was explored. Activation energies and pre-exponential factors for diffusion were calculated, demonstrating that the presence of a second solute significantly reduces the activation energy, leading to faster diffusion for most of the configurations. This effect is attributed to the reduction of repulsive or attractive forces and local lattice relaxations caused by the second solute atom. In addition, the study also revealed that the presence of a second solute atom of the same type can also alter the preferred diffusion pathways for both solutes. This complex interplay between solutes suggests that diffusion behavior in these materials is highly dependent on the specific solutes and their configurations within the lattice. This comprehensive understanding of diffusion mechanisms in refractory metals with interstitial solutes is crucial for their application in various technologies. Precise control over solute diffusion is crucial for optimizing these material properties and performances. Therefore, further research is required and of paramount importance to explore a wider range of solute combinations (H-N, N-O, H-O), composition (H_2O, N_2O, NO_2), and their behavior at varying concentrations.

Supplementary Information The online version contains supplementary material available at https://doi.org/10.1557/s43580-024-01028-3.

Acknowledgments The InterMaths Network: RealMaths Consortium at the Dipartimento di Ingegneria e Scienze dell'Informazione e Matematica, Universitá degli studi dell'Aquila, L'Aquila, Italy for the partnership. The authors would like to thank Prof. Bruno Rubino for the collaboration all this years in exchange students and staffs. This work was conducted using resources from the Lengau Cluster at the Centre for High-Performance Computing (CHPC) in Cape Town, South Africa, the CINECA high-performance computing (HPC) Center in Italy through project name IsCa5_VIMFIML and code HP10CURIS1, and the Hoffman2 shared cluster provided by the UCLA Institute for Digital Research and Education's Research Technology Group.

Author contributions Henry Elorm Quarshie contributed toward methodology, investigation, formal analysis, writing- original draft preparation, and writing- reviewing and editing. Henry Martin contributed toward project administration, conceptualization, methodology, formal analysis, and writing- reviewing and editing. Eric K. K. Abavare contributed toward methodology, formal analysis, and writing- reviewing and editing. Alessandra Continenza contributed toward methodology, formal analysis, and writing- reviewing and editing.

Funding No funds, grants, or other support were received.

Data availability The data required to reproduce these findings cannot be shared at this time due to technical limitations.

Code availability The code required to reproduce these findings cannot be shared at this time due to technical limitations.

Declarations

Conflict of interest All authors certify that they have no affiliations with or involvement in any organization or entity with any financial interest or non-financial interest in the subject matter or materials discussed in this manuscript.

Ethics approval Not applicable.

Consent to participate Not applicable.

Consent for publication Not applicable.

References

1. F. Habashi, Historical introduction to refractory metals. Miner. Process. Extr. Metall. Rev. **22**(1), 25–53 (2001). https://doi.org/10.1080/08827509808962488
2. G. Leichtfried, J.H. Schneibel, M. Heilmaier, Ductility and impact resistance of powder-metallurgical molybdenum-rhenium alloys. Metall. Mater. Trans. A **37**, 2955–2961 (2006). https://doi.org/10.1007/s11661-006-0177-9
3. Y. Wang, X. Wang, Q. Li, B. Xu, W. Liu, Atomistic simulations of carbon effect on kink-pair energetics of bcc iron screw

dislocations. J. Mater. Sci. **54**(15), 10728–10736 (2019). https://doi.org/10.1007/s10853-019-03564-y
4. X. Jiang, M. Wang, K. Schmidt, E. Dunlop, J. Haupt, W. Gissler, Elastic constants and hardness of ion-beam-sputtered TiNx films measured by Brillouin scattering and depth-sensing indentation. J. Appl. Phys. **69**(5), 3053–3057 (1991). https://doi.org/10.1063/1.348963
5. Y.-L. Liu, S. Jin, L. Sun, C. Duan, First-principles investigation on diffusion and permeation behaviors of hydrogen isotopes in molybdenum. Comput. Mater. Sci. **54**, 32–36 (2012). https://doi.org/10.1016/j.commatsci.2011.11.002
6. Y.-W. You, X.-S. Kong, X.-B. Wu, Q.F. Fang, J.-L. Chen, G.-N. Luo, C.S. Liu, Effect of vacancy on the dissolution and diffusion properties of hydrogen and helium in molybdenum. J. Nucl. Mater. **433**(1), 167–173 (2013). https://doi.org/10.1016/j.jnucmat.2012.09.025
7. G. Kresse, J. Hafner, Ab initio molecular dynamics for liquid metals. Phys. Rev. B **47**, 558–561 (1993). https://doi.org/10.1103/PhysRevB.47.558
8. G. Kresse, From ultrasoft pseudopotentials to the projector augmented-wave method. Phys. Rev. B Condens. Matter Mater. Phys. **59**(3), 1758–1775 (1999). https://doi.org/10.1103/PhysRevB.59.1758. (**Cited by: 61987**)
9. G. Kresse, J. Furthmüller, Efficient iterative schemes for ab initio total-energy calculations using a plane-wave basis set. Phys. Rev. B **54**, 11169–11186 (1996). https://doi.org/10.1103/PhysRevB.54.11169
10. M. Methfessel, A.T. Paxton, High-precision sampling for brillouin-zone integration in metals. Phys. Rev. B **40**, 3616–3621 (1989). https://doi.org/10.1103/PhysRevB.40.3616
11. D.D. Johnson, Modified broyden's method for accelerating convergence in self-consistent calculations. Phys. Rev. B **38**, 12807–12813 (1988). https://doi.org/10.1103/PhysRevB.38.12807
12. G. Henkelman, H. Jónsson, Improved tangent estimate in the nudged elastic band method for finding minimum energy paths and saddle points. J. Chem. Phys. **113**(22), 9978–9985 (2000). https://doi.org/10.1063/1.1323224
13. D.R. Trinkle, C. Woodward, The chemistry of deformation: how solutes soften pure metals. Science **310**(5754), 1665–1667 (2005). https://doi.org/10.1126/science.1118616
14. K. Hermann, Crystallography and surface structure: An introduction for surface scientists and nanoscientists (2017). https://doi.org/10.1002/9783527633296.ch2
15. C. Kittel, P. McEuen, P. McEuen, *Introduction to Solid State Physics*, vol. 8 (Wiley, New York, New York, 1996)
16. C. Duan, Y.-L. Liu, H.-B. Zhou, Y. Zhang, S. Jin, G.-H. Lu, G.-N. Luo, First-principles study on dissolution and diffusion properties of hydrogen in molybdenum. J. Nucl. Mater. **404**(2), 109–115 (2010). https://doi.org/10.1016/j.jnucmat.2010.06.029
17. H. Martin, E.K.K. Abavare, P. Amoako-Yirenkyi, Thermodynamic stable site for interstitial solute (n or o) in bcc refractory metals (mo and nb) using density functional theory. MRS Adv. **7**, 474 (2022). https://doi.org/10.1557/s43580-022-00280-9
18. D. Kandaskalov, L. Huang, J. Emo, P. Maugis, Carbon diffusion in bcc- and bct-fe: influence of short-range c-c pair interactions studied from first-principles calculations. Mater. Chem. Phys. **286**, 126159 (2022). https://doi.org/10.1016/j.matchemphys.2022.126159
19. Y.-L. Liu, F. Ding, G.-N. Luo, C.-A. Chen, Finite-temperature h behaviors in tungsten and molybdenum: first-principles total energy and vibration spectrum calculations. Nucl. Fus. **57**(12), 126024 (2017). https://doi.org/10.1088/1741-4326/aa8278
20. H. Mehrer, *Diffusion in Solids: Fundamentals, Methods, Materials, Diffusion-controlled Processes*, vol. 155, 1st edn. (Springer, Springer-Verlag, Berlin, 2007). https://doi.org/10.1007/978-3-540-71488-0
21. J.H. Evans, B.L. Eyre, The heat of solution and diffusivity of nitrogen in molybdenum. Acta Metall. **17**(8), 1109–1115 (1969). https://doi.org/10.1016/0001-6160(69)90055-8
22. C. Wert, C. Zener, Interstitial atomic diffusion coefficients. Phys. Rev. **76**, 1169–1175 (1949). https://doi.org/10.1103/PhysRev.76.1169
23. H. Katsuta, R.B. McLellan, K. Furukawa, Diffusivity and permeability of hydrogen in molybdenum. J. Phys. Chem. Solids **43**(6), 533–538 (1982). https://doi.org/10.1016/0022-3697(82)90104-4
24. C. Hartley, R. Wilson, Dislocation pinning effects in unalloyed molybdenum. Acta Metall. **11**(8), 835–845 (1963). https://doi.org/10.1016/0001-6160(63)90052-X
25. Z.-Q. Wang, Y.-H. Li, H. Gong, Q.-Y. Ren, F.-F. Ma, T. Liu, G.-H. Lu, H.-B. Zhou, Suppressing effect of carbon on oxygen-induced embrittlement in molybdenum grain boundary. Comput. Mater. Sci. **198**, 110676 (2021). https://doi.org/10.1016/j.commatsci.2021.110676
26. T.O. Oğurtani, E.M. Uygur, Diffusion of nitrogen in niobium, with special reference to temperature dependence of the activation energy. Trans. Jpn. Inst. Metals **13**(6), 396–399 (1972). https://doi.org/10.2320/matertrans1960.13.396